# Accumulation of radium in ferruginous protein bodies formed in lung tissue: association of resulting radiation hotspots with malignant mesothelioma and other malignancies

By Eizo NAKAMURA,[*1,†] Akio MAKISHIMA,[*1] Kyoko HAGINO[*1] and Kazunori OKABE[*2]

(Communicated by Takashi SUGIMURA, M.J.A.)

**Abstract:** While exposure to fibers and particles has been proposed to be associated with several different lung malignancies including mesothelioma, the mechanism for the carcinogenesis is not fully understood. Along with mineralogical observation, we have analyzed forty-four major and trace elements in extracted asbestos bodies (fibers and proteins attached to them) with co-existing fiber-free ferruginous protein bodies from extirpative lungs of individuals with malignant mesothelioma. These observations together with patients' characteristics suggest that inhaled iron-rich asbestos fibers and dust particles, and excess iron deposited by continuous cigarette smoking would induce ferruginous protein body formation resulting in ferritin aggregates in lung tissue. Chemical analysis of ferruginous protein bodies extracted from lung tissues reveals anomalously high concentrations of radioactive radium, reaching millions of times higher concentration than that of seawater. Continuous and prolonged internal exposure to hotspot ionizing radiation from radium and its daughter nuclides could cause strong and frequent DNA damage in lung tissue, initiate different types of tumour cells, including malignant mesothelioma cells, and may cause cancers.

**Keywords:** asbestos, ferruginous body, radium, hotspot radiation, malignant mesothelioma, cancer

## Introduction

Extensive epidemiological studies have linked asbestos exposure to the development of pulmonary diseases such as lung cancer and malignant mesothelioma.[1)–5)] Although commercial use of asbestos has been substantially limited since 1970, the long 20–40 year latency of mesothelioma makes it an ongoing societal health issue. Predicted numbers of deaths in the next 4 decades are 72,000 in the USA, 250,000 in Europe, 103,000 in Japan and 30,000 in Australia at predicted peak years of 2004 (USA), 2015–2020 (Europe), 2025 (Japan) and 2015 (Australia), respectively.[6)–8)] The lack of understanding of pathogenic mechanism for asbestos fibers causing pulmonary toxicity may have prevented the development of therapeutic and prophylactic remedies.

In post-mortem recovery, fine asbestos fibers can be observed either in histological sections of lung tissue in heavily exposed cases, or in separates following lung digestion.[9)] These fibers are frequently coated with iron-rich proteins such as ferritin and/or hemosiderin.[10)] Possible linkages between asbestos fibers, the formation of the iron-rich protein, the formation of toxic reactive oxygen species (ROS), DNA damage *in vitro* and apoptosis resistance, have been discussed, proposed and suggested in relation to asbestos-mediated pathogenesis including malignant mesothelioma development.[11)–14)] While the linkage is compelling, no specific mechanism appears to explain the development of malignant mesothelioma.

Trace-element abundance patterns are commonly used in geochemistry because the abundances of elements can be affected systematically or independently by geological processes because of differences in ion radius, charge and mass. By analogy, we set out to

[*1] The Pheasant Memorial Laboratory for Geochemistry and Cosmochemistry (PML), Institute for Study of the Earth's Interior, Okayama University, Tottori, Japan.

[*2] Yamaguchi Ube Medical Center, National Hospital Organization, Yamaguchi, Japan.

[†] Correspondence should be addressed: E. Nakamura, Institute for Study of the Earth's Interior, Okayama University, 827 Yamada, Misasa, Tottori 682-0193, Japan (e-mail: eizonak@misasa.okayama-u.ac.jp).

doi: 10.2183/pjab.85.229

Table 1. Patients characteristics and modes of asbestos in asbestos body (AB)

| Patient | | A | E | H | I | K | M |
|---|---|---|---|---|---|---|---|
| Age | | 65 | 65 | 63 | 59 | 51 | 61 |
| Sex | | Male | Female | Male | Male | Female | Male |
| Type of MPM*) | | Biphasic | Biphasic | Biphasic | Others | Epithelioid | Biphasic |
| Initial Symptom | | Cough | Chest pain | Cough | Pleural thickness | Chest pain | Chest pain |
| Occupation | | Quarrying industry | Insulation industry | Asbestos scrapper | Railway carriage builder | Post office | School teacher |
| Living place (prefecture) | | Yamaguchi | Fukuoka | Yamaguchi | Yamaguchi | Aichi | Shiga |
| Smoking | years<br>comment | 35<br>Quitted 6 months before operation | None | 40<br>Quitted 1 year before operation | None | None | 10<br>Quitted 30 years before operation |
| AB per dry lung | fiber $g^{-1}$ | $7.9 \times 10^3$ | $4.4 \times 10^5$ | $3.2 \times 10^5$ | $1.7 \times 10^4$ | $4.0 \times 10^3$ | $7.1 \times 10^2$ |
| Modes of asbestos in AB | | | | | | | |
| Amosite | % | 20 | 95 | 63 | 10 | 12 | 50 |
| Chrysotile | % | 0 | 0 | 0 | 0 | 0 | 0 |
| Crocidolite | % | 75 | 5 | 32 | 90 | 85 | 50 |
| Others (Silicious fiber, etc) | % | 5 | 0 | 5 | 0 | 2 | 0 |
| Crocidolite/Amosite | | 3.7 | 0.05 | 0.50 | 9.0 | 7.0 | 1 |
| Counted number | | 55 | 60 | 57 | 50 | 41 (few AB) | 2 (very few AB) |
| Volume of FB**) (qualitative) | | Large | Medium | Very large | Small | Medium | Medium |

*) MPM: Malignant pleural mesothelioma

**) FB: Ferruginous bodies

examine whether trace-element signatures or patterns might reveal an underlying cause of toxicity of inhaled asbestos fibers and dust particles associated with formation of ferruginous proteins in lung tissue. In order to characterize the trace-element behaviour during iron-storage protein (ferritin) formation, we carried out mineralogical and chemical analyses of asbestos bodies and coexisting fiber-free ferruginous protein bodies extracted from resected lungs of six individuals with malignant mesothelioma.

## Materials and methods

**Lung tissue digestion and asbestos body quantification.** Patients' characteristics are described in Table 1. Asbestos body quantification was performed by applying a modified technique of Smith and Naylor[15] at Yamaguchi Ube Medical Center. About 5 grams of surgically obtained representative, relatively normal, pulmonary parenchymal tissue were selected and removed. The sample of tissue was weighed, minced, dried, re-weighed, and transferred to a 50 ml centrifuge tube. Forty ml of bleach (CLEAN99K-200, Clean Chemical Co. Ltd., Osaka, Japan) containing 20% sodium hypochlorite and 5% potassium hydroxide was added to the tube. The tissue was allowed to digest for 24–48 hours. When the tissue was completely digested, the tube was centrifuged at 3000 rpm for 30 minutes and the supernatant liquid was aspirated, leaving about 1 ml of liquid covering the pellet. The pellet was re-suspended in 50 ml of deionized Milli-Q® pure water, and mixed well. These centrifugation, aspiration, re-suspension,

and mixing procedures were repeated three times. The final residue in water was quantitatively aliquoted for subsequent counting of asbestos bodies, mineralogical observation and chemical analysis.

A part of the final residue in water was filtered through a 0.45 μm membrane filter (ADVANTEC, Toyo Roshi Kaisha, Ltd., Tokyo, Japan). The filter was dried and then placed on microscope slide. The filter was dissolved using acetone vapour, and the cover slide was placed with a mounting medium, Entellan Neu (Merck KGaA, Darmstadt, Germany). The number of asbestos bodies on each filter was counted under phase-contrast optical microscope at 400-fold magnification.

**Analytical techniques for mineralogical description and major and trace element concentrations.** All the analyses were performed in a clean laboratory at the Pheasant Memorial Laboratory for Geochemistry and Cosmochemistry (PML), Institute for Study of the Earth's Interior, Okayama University at Misasa, Japan.[16)]

Another aliquot of the final residue was filtered and dried on a membrane filter, and the mineralogical description was carried out using Hitachi S-3100H scanning electron microscope (SEM) equipped with Horiba EMAX-7000 energy dispersive X-ray spectrometer (EDS).

The remaining aliquot was transferred into a quartz glass crucible and then placed in a muffle furnace with a quartz glass lid. The temperature was kept at 110 °C for 2 hours to achieve dryness and subsequently raised to 500 °C for 3 hours to ash proteins within the final residue. The ashed sample was then transferred into a Teflon PFA (perfluoroalkoxy copolymer) beaker with 3 ml of 0.06 M HCl, and agitated in an ultrasonic bath for 20 minutes. After centrifuging at 3000 rpm, the supernatant was collected as the leachate-1 (L-1). Then 3 ml of 1 M HCl was added to the residue and the same procedure was repeated, which yielded leachate-2 (L-2). The purpose of the two step leaching is to separate weakly embedded elements from strongly incorporated elements in proteins without decomposing asbestos. Then 0.6 ml of HF and 0.3 ml of $HClO_4$ were added into both the residue and the acid leachates (L-1 and L-2) and agitated in an ultrasonic bath for one day. The sample was then dried using method of Yokoyama *et al.*[17)] Fractions were then dissolved in 1 ml of 0.5 M $HNO_3$ and measured in 4 separate element groups: (i) trace elements-A (Li, Be, Rb, Sr, Y, Cs, Ba, La, Ce, Pr, Nd, Sm, Eu, Gd, Tb, Dy, Ho, Er, Tm, Yb, Lu, Pb, Th and U); (ii) trace elements-B (Cd, In, Tl and Bi); (iii) major and minor elements (Na, Mg, Al, P, K, Ca, Sc, V, Mn, Fe, Co, Ni, Cu, Zn and Ga); and (iv) $^{226}$Ra.

The trace elements-A were determined simultaneously by quadrupole-type inductively coupled plasma mass spectrometry (Q-pole type ICP-MS; Agilent 7500cs, Yokogawa Analytical Systems, Japan) using a pseudo-flow injection methods.[18)] The trace elements-B were determined by a modified method[19)] of ref. 18. For both cases, a conventional calibration curve method was employed, because matrix effects were negligible due to extremely small sample sizes. For determination of major and minor elements, sector field-type ICP-MS (ELEMENT, FinniganMAT, Germany) was used. Sodium, Mg, Al, P, Ca, V, Mn, Fe and Co were determined at medium mass resolution ($M/\Delta M = \sim 3000$), and K, Sc, Ni, Cu, Zn and Ga, at high resolution ($M/\Delta M = \sim 7500$).

Radium-226 was determined by multi-collector (MC) ICP-MS (NEPTUNE, ThermoElectron, Germany) using a retarding potential quadrupole secondary electron multiplier (RPQ-SEM).[20)] The sensitivity of the MC-ICP-MS was typically 30 count $s^{-1}$ $fg^{-1}$ ml with background of 15 count $s^{-1}$ with sample consumption of 0.1 ml for 60 s data integration. Three-sigma detection limit was 0.06 fg $ml^{-1}$. A calibration curve method was applied using a diluted solution of NIST (National Institute for Standard and Technology) 4966 $^{226}$Ra solution as standard, because matrix effects and molecular interferences were considered to be negligible at the concentration levels of this study.

The major, minor and trace elements and $^{226}$Ra of three asbestos standards (chrysotile from California: JAWE131; amosite from Transvaal: JAWE231; crocidolite from Cape: JAWE331; issued from Japan Association for Working Environment measurement) were also determined with the methods described elsewhere.[18),19)] Radium-226 was measured in the similar manner as the separates from lung tissues without chemical separation of $^{226}$Ra. However, it was below the detection limit. This clearly indicates that matrix of asbestos minerals do not cause ''ghost signals'' or ''molecular ions'' at mass 226, supporting the validity of the $^{226}$Ra signals in the analysis of separates from lung samples and proteins.

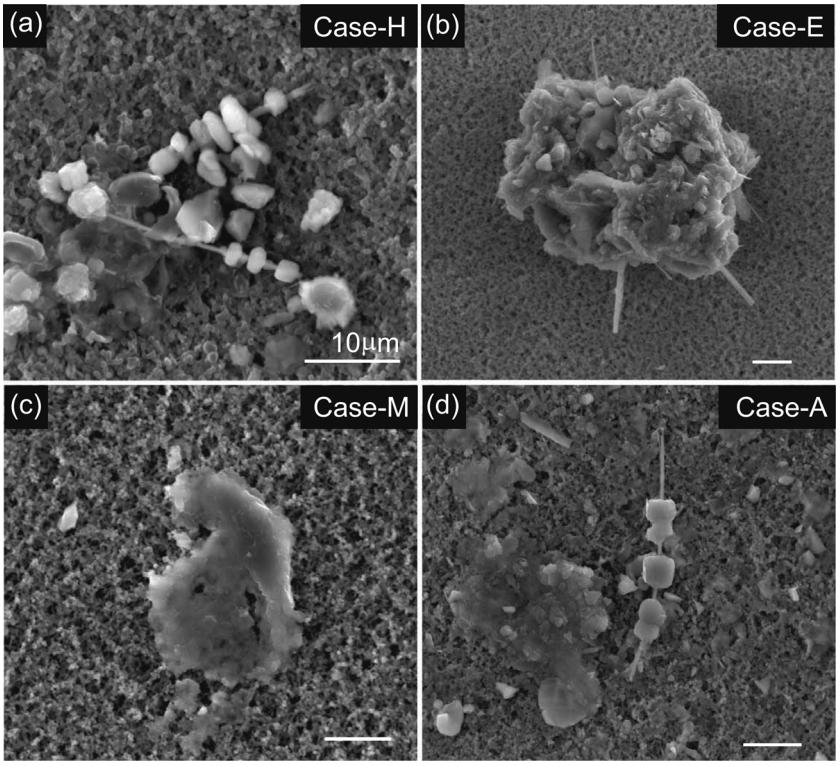


Fig. 1. Scanning electron microscopic images of representative asbestos bodies and ferruginous proteins extracted from the lung tissues associated with human malignant mesothelioma. **a,** Asbestos bodies with beaded and fragmented ferruginous proteins isolated from Case-H, an asbestos scrapper. Cores of the bodies are crocidolite (upper) and amosite (lower). Fiber-free amorphous ferruginous protein bodies were also accompanied with asbestos bodies. **b,** Complex asbestos body consisting of intertwined amosite fibers and ferruginous proteins extracted from Case-E, an insulator industry worker. Adhering ferruginous proteins are likely aggregates of malformed proteins, indicating multi-stage development of proteins. **c,** A ferruginous protein body which does not contain asbestos fiber. Texture of the protein body resembles those of amorphous protein bodies in **a, b** and **d**. Asbestos body concentration of Case-M is extremely low (700 fibers $g^{-1}$ dry lung) and the separates are mostly this type of ferruginous protein. **d,** Asbestos body with core of amosite fiber and fiber-free amorphous ferruginous protein bodies from Case-A. Scale bars correspond to 10 μm.

## Results and discussion

**Mineralogical description.** Asbestos bodies with coexisting fiber-free ferruginous protein bodies extracted from lung samples of six malignant mesothelioma patients showed a range in morphology (Fig. 1). Asbestos fibers with diameter $<200$ nm were often coated by adhering protein aggregates, although some fibers extracted were not associated with protein bodies probably due to their detachments during extraction processes. These asbestos bodies commonly appear beaded, segmented or dumbbell-shaped as described in the previous studies.[9),10)] The proteins are characterized by high Fe and P concentrations and show reddish brown colour under the optical microscope, consistent with the general characteristic of ferritin.[21)] Ferruginous protein bodies without fibers show aggregate textures consisting of either amorphous or irregularly crystalline materials (Fig. 1a, c and d). These materials have high concentrations of Fe, P and Ca with traces of Mg, S and few other elements. Fiber-free ferruginous protein bodies show either dark-brown or reddish brown colour. This colour may result from heterogeneous conversion from ferritin to hemosiderin under oxidative condition in lung.[10)] It is noted that the amounts of fiber-free ferruginous protein bodies extracted from cigarette smokers (Case-A, -H and -M) were significantly larger than non-smokers (Table 1).

The observed asbestos fibers were iron-rich amphiboles such as crocidolite (riebeckite, $Na_2 \cdot Fe^{2+}{}_3Fe^{3+}{}_2Si_8O_{22}(OH)_2$) and amosite (grunerite, $Fe^{2+}{}_7Si_8O_{22}(OH)_2$). No chrysotile (iron-poor serpentine) fibers were found. Volumetric analysis (Table 1) indicates a highly variable crocidolite/amosite ratio, ranging from 0.05 to 9.0. This may imply that these patients were exposed to asbestos fibers from different sources. The mineralogical analysis indicates that iron-poor chrysotile fibers were not involved in the pathogenesis of malignant mesothelioma for these six patients. This is consistent with the observation that the formations of ferruginous proteins on chrysotile fibers are generally very scarce.[22)–24)] Glass fibers and unidentifiable silicate fibers without protein coatings were also observed (Table 1).

**Chemical compositions.** Forty-four elements were measured for asbestos bodies and coexisting fiber-free ferruginous protein bodies from six malignant mesothelioma patients along with three asbestos standards (chrysotile, amosite and crocidolite). The results are accessible from Data Information (DI-Tables 1-4), http://depo.misasa.okayama-u.ac.jp/suppinfo/. In order to derive quantitative trace element concentrations in the material objects, an accurate estimate of the relative masses is necessary. By assuming that all elements are contained in asbestos bodies, the major and trace element concentrations were estimated by the inferred sample weights based on average volumes and densities of core fiber and adhering proteins together with numbers of asbestos bodies obtained by counting (Table 1, DI-Table 1). Concentrations of major elements such as Na, Mg, Al, P, K, Ca, Mn and Fe obtained with this method are unrealistically high, primarily due to inadequate sample weights used for the concentrations determination. Additional errors may originate in the separated residues other than asbestos bodies being present. Because of the lack of correlation between asbestos body counts and Fe contents normalized to dry lung weight (Fig. 2), there must be some additional components other than asbestos bodies. The elevated Fe signal suggests that it is derived from iron-storage proteins such as ferritin and hemosiderin which is considered to be altered ferritin either associated with or not associated with asbestos fibers.[10)] This suggestion is semi-quantitatively supported by the fact that the ashing-processed samples at 500 °C were red caused by the formation of $Fe_2O_3$ from ferruginous protein. The ashing temperature does not decompose silicate minerals so that it is likely that the most of iron in the samples were derived from the iron-storage proteins, which formed ferruginous protein bodies. In comparison, the contribution to the trace element concentrations from asbestos fibers is negligible considering their sizes and concentrations.

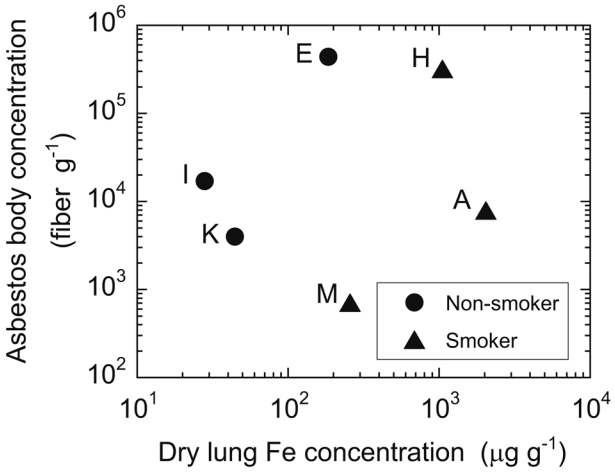


Fig. 2. Asbestos body concentration versus Fe concentration of extracted ferruginous proteins bodies from lung tissues. Iron concentration is normalized to mass of dry lung sample used for asbestos body extraction. Case-E, -I and -K were non-smokers. Case-A and -H had been smoking cigarette for 35 and 40 years and stopped smoking 6 and 12 months before operation, respectively. Case-M had smoked for approximately 10 years, and then quitted 30 years before operation. It was declared that Case-E, -H, and -I had been involved in asbestos exposure. Meanwhile, the other cases did not show clear association with asbestos exposure.

In order to establish more accurately the concentration levels in the separates, we assumed that all protein separates consist of ferritin, which has a capacity of up to 4000 to 4500 Fe atoms/molecule in its interior.[25)] As such, we normalized the trace element concentrations to the Fe concentration of 27 wt.% in ferritin. Hemosiderin may be a converted product from ferritin in oxidative lung condition.[10)] If hemosiderin is the ferruginous protein, the apparent elemental abundances will increase compared with those in the case of ferritin. In order to facilitate comparison of concentrations, thirty-three trace elements are normalized to the element abundances in hypothetical Earth's primitive mantle, the composition of a whole silicate Earth after core formation (PM-normalized).[26)] In addition the P and Fe con-

centrations, which are the major elements in ferritin and hemosiderin, are also shown.

We carried out step-wise acid leaching experiment after ashing the separates at 500 °C as described in Materials and methods. All analyses of L-1 (leachates with dilute 0.06M HCl), have similar PM-normalized trace-element patterns with highly elevated abundances of large radius ionic elements and light rare earth elements (LREEs) (to left of Fig. 3a). Moreover, significant positive anomalies of Ra, Ba, Pb, Cd and Zn relative to their neighbouring elements are apparent. The patterns from the second leachates (L-2), with 1 M HCl, exhibit more variability than those from the first leachates, especially in heavy rare earth elements (HREEs), while retaining substantial enrichments of Ra, Pb and Cd (Fig. 3b). This greater variability might be attributed to the difference in the proportion of ferritin and hemosiderin proteins caused by different resistance of ashing products to acid concentration during sample preparation. The PM-normalized patterns of the bulk separate samples (L-1 + L-2 + residue) closely resemble those of 0.06 M leachates with similar abundance levels (within one order of magnitude) for REE of different samples (Fig. 3c), which are substantially smaller than the variation (two orders of magnitude) of PM-normalized patterns normalized to the weight of dry sample used for the separation (Fig. 3d).

These observations imply that elemental abundances in the 0.06 M leachates are markedly higher than those in the bulk separates from lung samples, and thus the main reservoir of these elements is probably ferruginous protein such as ferritin. Moreover, U abundances are substantially higher than HREE (e.g., Lu) in PM-normalized diagram (Fig. 3). This observation also favours ferritin as the host because of a very high affinity of U to apoferritin.[27] It is, therefore, suggested that ferritin in lung tissue incorporates preferentially ions with larger radii such as $Rb^{+}$, $Ra^{2+}$, $Ba^{2+}$, $UO_2^{2+}$ and $Th^{4+}$. This suggestion is also supported by the systematic increase of $LREE^{3+}$ relative to $HREE^{3+}$ with increasing iron abundance. Furthermore, the protein tends to incorporate $Cd^{2+}$ and $Zn^{2+}$ as occurs in metal-binding proteins[28] like metallothionein, which is thought to be involved in regulation of physiological metals (Cu and Zn) providing protection against metal toxicity and oxidative stress.[29),30]

These chemical characteristics may be attributed to the unique molecular structure of ferritin,

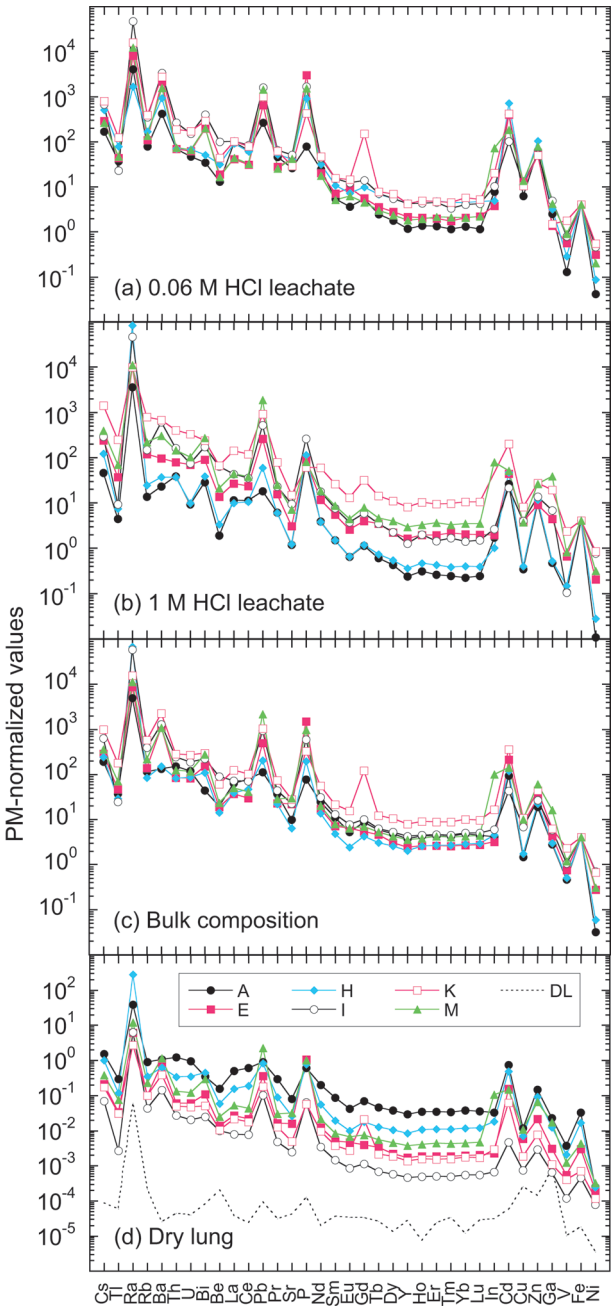


Fig. 3. Primitive-mantle-normalized trace-element patterns of asbestos bodies and ferruginous protein bodies. **a,** First leachates with 0.06 M HCl. **b,** Second leachates with 1 M HCl. **c,** Bulk compositions (**a**+**b**+residues). In **a, b** and **c,** element abundances are normalized to 27 wt% of Fe (4000 Fe atoms retained in one ferruginous protein, ferritin).[31] **d,** Bulk compositions normalized to mass of dry lung used for the asbestos body extraction. Broken line indicates detection limits of the method of analyses. The PM-normalized abundances are depicted as pattern for which the trace elements are arranged in order of their incompatibilities to the silicate mantle increasing from left to right.[26]

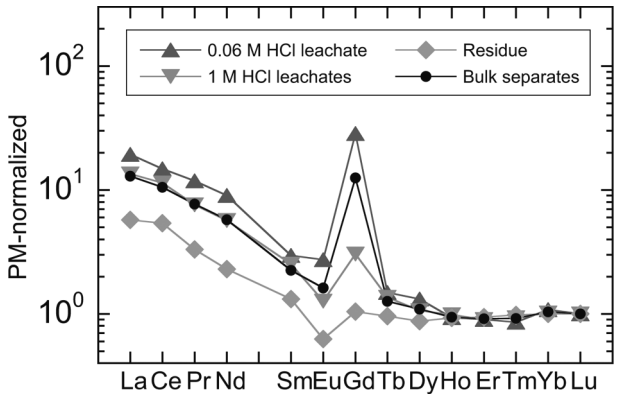


Fig. 4. Primitive-mantle-normalized REE patterns of stepwise acid leachates of separates from Case-K. Primitive-mantle-normalized REE patterns are re-normalized to Lu. A strong positive Gd-spike observed for bulk composition is more emphasized in the first leachate with 0.06 M HCl and weakened with the second leachate with 1 M HCl. Residue showed no Gd anomaly, but instead showed negative Eu anomaly.

which is well suited to its intercellular role as an iron-storage compound. The protein component without iron, apoferritin, is characterised by a hollow spherical protein shell (outer diameter 12–13 nm, inner 7–8 nm, Mass $5 \times 10^5$ Dalton) composed of 24 polypeptide chains and capable of storing $Fe^{3+}$ atoms as a microcrystalline core of ferrihydrite (a ferric oxyhydroxide).[31] Because of its reactivity and large specific surface area, ferrihydrite is also believed to be one of the most important adsorbents and/or co-precipitator of minor elements in surface and groundwater systems.[32),33] It is, thus, likely that large radius ions are incorporated into the ferrihydrite precipitated in the ferritin core (ferritin-ferrihydrite). Furthermore, there are preferential uptakes of Ra, Ba, Pb, Cd and Zn, which are the remarkable chemical characteristics of ferritin at physiological pH under oxidising conditions in the lung tissue.

**Gadolinium anomaly in trace element pattern.** It is notable that Case-K has a positive gadolinium (Gd) anomaly in PM-normalized pattern (Fig. 3). This feature is seen even more clearly in the PM-normalized REE patterns, re-normalized to Lu (Fig. 4). The Gd anomaly (Gd* value) decreased from 15 to 1 with successive acid leaching steps together with decreasing La/Lu ratios, and decreasing P and Fe abundances (DI-Table 2). Geochemically and crystal chemically, a Gd anomaly is not expected and was perplexing because the REEs exist in +3 valence state over a wide range of oxygen fugacity except for Ce and Eu. Furthermore, ionic radius, which decreases progressively from $La^{3+}$ (115 pm) to $Lu^{3+}$ (93 pm), is the characteristic that governs smooth changes of their relative behaviour.[34] This situation was clarified through consultation with the case history.

About 3 months before the surgery to remove the tumour, Case-K was examined by a magnetic resonance imaging (MRI) system and the contrast agent used for this procedure was a Gd-rich compound, gadpentetate dimeglumine (Gd-DTPA). The plasma half-life of Gd from this compound is approximately 1 hour, and thus nearly 100% of the Gd injected intravenously is excreted within 24 hours.[35] However, the large Gd anomaly observed in Case-K is serendipitously an important independent control experiment and suggests that elements such as REE, Ra, Ba, Pb, Cd and Zn can be immediately adsorbed or co-precipitated with extremely high efficiency and persist in a fixed form. In this case, trace elements are associated with ferrihydrite in the ferritin deposited around asbestos and asbestos-free ferruginous protein bodies in human lung tissue. It is well known that ferritin plays a key role in iron metabolism with iron detoxification and iron reservation. The importance of these functions is emphasized by ferritin's ubiquitous distribution among species.[25] Our observation probably suggests that the ferritin may also be an efficient scavenger of toxic heavy metals and large radius ions, which can be excreted from kidney. Specific proteolytic enzyme likely functions in kidney through ferritin metabolism because of extremely high excretion rate of Gd.

**Radium enrichment and ionizing radiation hotspot in lung.** A critical finding of this study is the anomalously high concentrations of radioactive radium ($^{226}$Ra) in ferruginous protein bodies ranging from 0.03 to 0.4 ng $g^{-1}$ (see DI-Table 3). These abundances are equivalent to enrichments of $10^6$ to $10^7$ relative to the seawater composition.[36] $^{226}$Ra is the fifth daughter nuclide of the $^{238}$U-$^{206}$Pb decay chain and has a half-life of 1600 years. It decays to $^{222}$Rn emitting high energy (4.871 MeV) alpha (α) particles, followed by spontaneous α-decay of $^{222}$Rn (3.8 days, 5.490 MeV), $^{218}$Po (3.1 minutes, 6.003 MeV) and $^{214}$Po ($1.64 \times 10^{-4}$ seconds, 7.687 MeV) to $^{210}$Pb (22.3 years). $^{222}$Rn is an inert gas, but is likely to be retained in the ferritin-ferrihydrite structure because $^{226}$Ra decays within the solid mass

of ferritin-ferrihydrite in lung. Thus, the integrated α-particles emitted through the decay chain from $^{226}$Ra to $^{210}$Pb, are highly effective in damaging tissues within the lung, in comparison to the case of inhaled radon progeny decay which have been previously proposed for the association of radon and lung cancer.[37)]

The high-energy α particles are likely to penetrate the ambient pulmonary cells, in which ionizing radiation could induce many forms of DNA damage directly and/or indirectly. This process could result in formation of highly reactive free radicals, base damage, DNA-protein cross-links, single-strand breaks, and double-strand breaks.[38)–40)] Ionizing radiation can further induce direct mutations[41)] and chromosome aberrations.[42)] Continuous internal exposure to ionizing radiation at fixed points, where ferritin-ferrihydrite forms and remains in the lung tissue, should more densely and frequently induce DNA damages than the case of inhalation of radon gas and could thus be extremely carcinogenic.

**Formation of ferruginous body in lung and a possible carcinogenic mechanism.** The formation of ferruginous protein bodies has been previously considered to be a protective mechanism of the host to mitigate the toxicity of asbestos fibers.[43)–45)] In contrast, it has also been suggested that iron in the protein deposited on amosite and crocidolite may contribute to the generation of the ROS potential for carcinogenesis in the lung.[46),47)] Although the physiological role and mechanism of formation of ferruginous bodies have not been fully elucidated, it is generally accepted that the redox-reactive iron in asbestos can induce synthesis of apoferritin after which process iron can be stored in this protein as ferritin after oxidation of the metal cation to ferric iron ($Fe^{3+}$).[25),48),49)] This series of reactions is likely to occur near the surface of iron-rich asbestos fiber.[10),50)] In recent *in vitro* experiments, the ferritin induction was hampered by iron chelation of crocidolite, and the induction by iron-poor chrysotile was clearly less than crocidolite.[12)] These investigations are consistent with the facts that ferruginous protein formation on chrysotile fibers is very rare in all the tissue specimens observed from persons who had been exposed only to this type of fiber.[21)] The occurrence of protein-coated fibers was also extremely rare for chrysotile.[51)] The observations made here are also consistent with these conclusions.

As described earlier, significant amounts of fiber-free ferruginous protein bodies were extracted from all patients. In addition, as shown in Fig. 2, cigarette smokers show higher iron concentrations than non-smokers. Because most of the iron and trace elements analyzed were from ferruginous protein bodies, the high iron concentrations in cigarette smokers may have resulted from excess iron deposition by continuous smoking.[52)] In support of this interaction, cigarette smoking, iron welding, and the mining of iron ore can be associated with elevations in both metal concentrations and coated fibers.[53),54)] The deposited iron might have induced the formation of ferruginous protein bodies in lung without asbestos fibers. This suggestion means that iron-rich materials deposited in lung tissue either breaks down to produce ferritin or act as nucleation sites for the protein, irrespective of shape and mineral phase. If this were the case, introduction of any iron-containing dust particles by inhalation will increase the risk of resulting in internal ionizing radiation of Ra and its daughter nuclides as carcinogenic factors in lung tissues by increasing the probability for the formation of ferritin, where Ra is stored. This proposed model may provide further insight into the interpretation of epidemiologic data of underground miners, which linked radon to lung cancer in smokers and non-smokers.[55),56)] Miners of iron and uranium ores generally work in dusty environments with high metal concentrations, thus facilitating the formation of ferruginous protein bodies in their lungs. These bodies will provide sites for adsorbing Ra to dangerously high levels.

Accumulated particles enriched in iron, which have survived from alveolar macrophage due to the excess inhalation of dust and continuous smoking, induce the formation of ferritin under unique physiological condition in the lung tissues. Along with the formation of ferritin, ferrihydrite precipitates in the ferritin molecule. The ferritin-ferrihydrite coprecipitates and adsorbs large radius ions with extreme enrichments of Ra from iron-rich particles and ambient tissue fluids. Accumulation of Ra in ferritin-ferrihydrite, which constructs ferruginous protein body, will become a hotspot of intense ionizing radiation from the Ra decay chain.

These hotspots of Ra ionizing radiation could continue to induce strong and frequent DNA damage in ambient lung cells, and could initiate different types of tumour cells, including malignant mesothelial cells. Tumour cells might be detached from tissues and become entrained into the bloodstream as

circulating tumour cells (CTCs), which may constitute seeds for subsequent growth of additional tumours (metastasis) in different tissues,[57),58)] implying that the Ra ionizing radiation associated with ferruginous protein bodies as observed here might play a critical role as a carcinogenic factor. The development of malignant mesothelioma may be one of the cases initiated in the lung tissues by the Ra ionizing radiation. This mechanism explains the long gestation period, and long pathway from the asbestos fibers in the lung to the mesothelioma. It is, therefore, clear that asbestos fibers themselves may be not substantial carcinogenic source, but only the iron-rich asbestos minerals such as amosite and crocidolite coated by ferruginous proteins would increase incidence of cancers. Furthermore, the effect of these materials may not be limited to malignant mesothelioma but also to a variety of cancers. The onset of cancer can be determined by exposure to iron-rich particles, numbers of particles accumulated over time, development of ferritin-ferrihydrite, and accumulation of Ra in ferruginous protein body in lung. These factors are then exaggerated or mitigated by genetic predisposition.

## Acknowledgements

We are deeply indebted to T. Sugimura, M.J.A. and I. Kushiro, M.J.A. for reviewing this paper with very helpful comments. We also appreciate Editor and four anonymous reviewers for their critical comments and suggestions that significantly improved the quality of paper. We thank Mr. K. Kuroda for his valuable technical assistance with the lung digestion and asbestos body counting. E.N. appreciates T. Takahashi, N. Kobayashi, K. Ashida and T. Katsura for helping understand biomedical science. We are grateful to T. Ireland, B. Mysen, N. Shimizu, D. Fraser and K. Yamashita for improving the manuscript with valuable comments. We thank K. Kobayashi and N. Tomioka for discussion and their technical help. A. Sarbadhikari and S. Malaviarachchi are thanked for brushing-up the draft. This study was carried out under approval by the Ethics Committee of Yamaguchi Ube Medical Center, National Hospital Organization of Japan.

## References

1) Mossman, B.T., Bignon, J., Corn, M., Seaton, A. and Gee, J.B.L. (1990) Asbestos: Scientific developments and implications for public policy. Science **247**, 294–301.
2) Jaurand, M.C. (1997) Mechanism of fiber-induced genotoxicity. Environ. Health Perspect **105**, 1073–1084.
3) Kamp, D.W. and Weitzman, S.A. (1999) The molecular basis of asbestos induced lung injury. Thorax **54**, 638–652.
4) Roggli, V.L., Sharma, A., Butnor, K.J., Sporn, T. and Vollmer, R.T. (2002) Malignant mesothelioma and occupational exposure to asbestos: A clinicopathological correlation of 1445 cases. Ultrastruct. Pathol. **26**, 55–65.
5) Upadhyay, D. and Kamp, D.W. (2003) Asbestos-induced pulmonary toxicity: Role of DNA damage and apoptosis. Exp. Biol. Med. **228**, 650–659.
6) Price, B. and Ware, A. (2004) Mesothelioma trends in the United States: an update based data on Surveillance, Epidemiology, and End Results Program for 1973 through 2003. Am. J. Epidemiol. **159**, 107–112.
7) Robinson, B.W.S. and Lake, R.A. (2005) Medical progress—Advances in malignant mesothelioma. New Engl. J. Med. **353**, 1591–1603.
8) Morinaga, K., Kishimoto, T., Sakatani, M., Akira, M., Yokoyama, K. and Sera, Y. (2001) Asbestos-related lung cancer and mesothelioma in Japan. Ind. Health **39**, 65–74.
9) Godleski, J.J. (2004) Role of asbestos in etiology of malignant pleural mesothelioma. Thorac. Surg. Clin. **14**, 479–487.
10) Ghio, A.J., Churg, A. and Roggli, V.L. (2004) Ferruginous bodies: Implications in the mechanism of fiber and particle toxicity. Toxicol. Pathol. **32**, 643–649.
11) Carbone, M., Kratzke, R.A. and Testa, J.R. (2002) The pathogenesis of mesothelioma. Semin. Oncol. **29**, 2–17.
12) Aung, W., Hasegawa, S., Furukawa, T. and Saga, T. (2007) Potential role of ferritin heavy chain in oxidative stress and apoptosis in human mesothelial and mesothelioma cells: implications for asbestos-induced oncogenesis. Carcinogenesis **28**, 2047–2052.
13) Kasai, H. and Nishimura, S. (1984) DNA damage induced by asbestos with the presence of hydrogen peroxide. Gann **75**, 841–844.
14) Christensen, B.C., Godleski, J.J., Marsit, C.J., Houseman, E.A., Lopez-Fagundo, C.Y., Longacker, J.L. *et al.* (2008) Asbestos exposure predicts cell cycle control gene promoter methylation in pleural mesothelioma. Carcinogenesis **29**, 1555–1559.
15) Smith, M.J. and Naylor, B. (1970) A method for extracting ferruginous bodies from sputum and pulmonary tissue. Am. J. Clin. Pathol. **58**, 250–254.
16) Nakamura, E., Makishima, A., Moriguti, T., Kobayashi, K., Sakaguchi, C., Yokoyama, T. *et al.* (2003) Comprehensive geochemical analyses of small amounts (100 mg) of extraterrestrial samples for the analytical competition related to the sample-return mission, MUSES-C. Inst. Space Astronaut. Sci. Rep. SP. **16**, 49–101.
17) Yokoyama, T., Makishima, A. and Nakamura, E.

(1999) Evaluation of the coprecipitation of incompatible trace elements with fluoride during silicate rock dissolution by acid digestion. Chem. Geol. **157**, 175–187.

18) Makishima, A. and Nakamura, E. (2006) Determination of major, minor and trace elements in silicate samples by ICP-QMS and ICP-SFMS applying isotope dilution-internal standardization (ID-IS) and multi-stage internal standardization. Geostand. Geoanal. Res. **30**, 245–271.

19) Makishima, A., Kitagawa, H. and Nakamura, E. Simultaneous determination of Cd with In, Tl and Bi by isotope dilution-internal standardization ICP-QMS using externally measured $MoO^+/Mo^+$ ratios (submitted to Geostand. Geoanal. Res.).

20) Makishima, A., Chekol, T.A. and Nakamura, E. (2008) Precise measurement of $^{228}Ra/^{226}Ra$ for $^{226}Ra$ determination employing total integration and simultaneous $^{228}Th$ correction by multicollector ICP-MS using multiple ion counters. J. Anal. At. Spectrom. **23**, 1102–1107.

21) Granick, S. (1946) Ferritin: its properties and significance for iron metabolism. Chem. Rev. **38**, 379–403.

22) Pooley, F.D. (1972) Asbestos bodies, their formation, composition and character. Environ. Res. **5**, 363–379.

23) Roggli, V.L., Pratt, P.C. and Brody, A.R. (1986) Asbestos content of lung tissue in asbestos associated diseases: a study of 110 cases. Br. J. Ind. Med. **43**, 18–28.

24) Dodson, R.F., O'Sullivan, M., Corn, C.J., McLarty, J.W. and Hammar, S.P. (1997) Analysis of asbestos fiber burden in lung tissue from mesothelioma patients. Ultrastruct. Pathol. **21**, 321–336.

25) Harrison, P.M. and Arosio, P. (1996) Ferritins: molecular proteins, iron storage function and cellular regulation. Biochim. Biophys. Acta **1275**, 161–203.

26) McDonough, W.F. and Sun, S-s. (1995) The composition of the Earth. Chem. Geol. **120**, 223–253.

27) Hainfeld, J.F. (1992) Uranium-loaded apoferritin with antibodies attached: Molecular design for uranium neutron-capture therapy. Proc. Natl. Acad. Sci. USA **89**, 11064–11068.

28) Price, D.J. and Joshi, J.G. (1983) Ferritin, Binding of beryllium and other divalent metal ions. J. Biol. Chem. **25**, 10873–10880.

29) Margoshes, M. and Vallee, B.L. (1957) A cadmium protein from equine kidney cortex. J. Am. Chem. Soc. **79**, 4813–4814.

30) Kumari, M.V., Hiramatsu, M. and Ebadi, M. (1998) Free radical scavenging actions of metallothionein isoforms I and II. Free Rad. Res. **29**, 93–101.

31) Harrison, P.M., Fishbach, F.A., Hoy, T.G. and Haggis, G.H. (1967) Ferric oxyhydroxide core of ferritin. Nature **216**, 1188–1190.

32) Krauskopf, K.B. (1955) Factors controlling the concentration of thirteen rare metals in seawater. Geochim. Cosmochim. Acta **9**, 1–24.

33) Jambor, J.L. and Dutrizac, J.E. (1998) Occurrence and constitution of natural and synthetic ferrihydrite, a widespread iron oxyhydroxide. Chem. Rev. **98**, 2549–2585.

34) Shannon, R.D. and Prewitt, C.T. (1969) Effective ionic radii in oxides and fluorides. Acta Cryst. **B25**, 925–946.

35) Yoshikawa, H., Nishikawa, J., Kosaka, N., Okada, Y., Aoki, S., Itoh, M. *et al.* (1986) Clinical phase I study of Gd-DTPA as MRI contrast agent. Jpn. J. Med. Imag. **6**, 959–969.

36) Broecker, W.S., Li, Y.H. and Cromwell. J. (1967) Radium-226 and radon-222: Concentration in Atlantic and Pacific Oceans. Science **158**, 1307–1301.

37) James, A.C. (1988) Lung dosimetry. *In* Radon and Its Decay Products in Indoor Air (eds. Nazaroff, W.W. and Nero, A.V. Jr.). Wiley, New York, pp. 259–309.

38) Ward, J. F. (1998) Nature of Lesions Formed by Ionizing Radiation. *In* DNA Damage and Repair, Vol. II. DNA repair in higher eukaryotes (eds. Nickoloff, J.A. and Hoekstra, M.F.). Humana Press, Totowa, pp. 65–84.

39) Little, J.B. (2000) Radiation carcinogenesis. Carcinogenesis **21**, 397–404.

40) Huang, L., Snyder, A.R. and Morgan, W.F. (2003) Radiation-induced genomic instability and its implications for radiation carcinogenesis. Oncogene **22**, 5848–5854.

41) Liber, H. L. and Phillips, E.N. (1998) Interrelationships between radiation-induced mutations and modifications in gene expression linked to cancer. Crit. Rev. Eukaryot. Gene Exp. **8**, 257–276.

42) Cornforth, M.N. (1998) Radiation-Induced Damage and The Formation of Chromosomal Aberrations. *In* DNA Damage and Repair, Vol. II. DNA repair in higher eukaryotes (eds. Nickoloff, J. A. and Hoekstra, M.F.). Humana Press, Totowa, pp. 559–585.

43) Mace, M.L., McLemore, T.L., Roggli, V., Brinkley, B.R. and Greenberg, S.D. (1980) Scanning electron microscopic examination of human asbestos bodies. Cancer Lett. **9**, 95–104.

44) Morgan, A. and Holmes, A. (1985) The enigmatic asbestos body: its formation and significance in asbestos-related disease. Environ. Res. **38**, 283–292.

45) Ghio, A.J., Le Furgy, A. and Roggli, V.L. (1997) *In vivo* accumulation of iron crocidolite is associated with decrements in oxidant generation by the fiber. J. Toxicol. Environ. Health **50**, 125–142.

46) Fubini, B., Barcelo, F. and Ortero-Arean, C. (1997) Ferritin adsorption on amosite fibers: possible implications in the formation and toxicity of asbestos bodies. J. Toxicol. Environ. Health **52**, 101–110.

47) Lund, L.G., Williams, M.G., Dodson, F.R. and Aust, A.E. (1994) Iron associated with asbestos bodies is responsible for the formation of single-strand breaks in phi-xl 174-Rfi DNA. Occup. Environ. Med. **51**, 200–204.

48) Ghio, A.J., Stonehuerner, J., Richards, J. and Devlin, R.B. (2008) Iron hemostasis in the lung following asbestos exposure. Antioxidants & Redox Signaling **10**, 371–377.

49) Lewin, A., Moore, G.R. and Le Brum, N.E. (2005) Formation of protein-coated iron minerals. Dalton Trans., 3597–3610, doi:10.1039/b506071k.
50) Hardy, J.A. and Aust, A.E. (1995) Iron in asbestos chemistry and carcinogenicity. Chem. Rev. **95**, 97–118.
51) Murai, Y., Kitagawa, M. and Hiraoka, T. (1995) Asbestos body formation in the human lung: Distinctions by type and size. Arch. Environ. Health **50**, 19–25.
52) Thompson, A.B., Bohling, T., Heires, A., Linder, J. and Rennard, S.I. (1991) Low respiratory tract iron burden is increased in association with cigarette smoking. J. Lab. Clin. Med. **117**, 493–499.
53) Churg, A. and Warnock, M.L. (1977) Analysis of the cores of ferruginous (asbestos) bodies from the general population. 1. Patients with and without lung cancer. Lab. Invest. **37**, 280–286.
54) McGowan, S.E. and Henley, S.A. (1988) Iron and ferritin contents and distribution in human alveolar macrophages. J. Lab. Clin. Med. **111**, 611–617.
55) Samet, J.M. (1989) Radon and lung cancer. J. National Cancer Institute, **81**, 745–757.
56) Lubin, J.H., Boice, J.D., Edling, C., Hornung, R.W., Howe, G.R., Kunz, E. *et al.* (1995) Lung-cancer in radon-exposed miners and estimation of risk from indoor exposure. J. Natl. Cancer Inst. **87**, 817–827.
57) Poste, G. and Fidler, I.J. (1980) The pathogenesis of cancer metastasis. Nature **283**, 139–146.
58) Nagrath, S., Sequist, L.V., Maheswaran, S., Bell, D.W., Irimia, D., Ulkus, L. *et al.* (2007) Isolation of rare circulating tumour cells in cancer patients by microchip technology. Nature **450**, 1235–1239.

(Received Apr. 27, 2009; accepted May 19, 2009)